Supplemental Material: Probe knots and Hopf insulators with ultracold atoms

Dong-Ling Deng,[1,2,3,*] Sheng-Tao Wang,[1,4,3] Kai Sun,[1] and L.-M. Duan[1,3]

[1]*Department of Physics, University of Michigan, Ann Arbor, Michigan 48109, USA*
[2]*Condensed Matter Theory Center and Joint Quantum Institute, Department of Physics, University of Maryland, College Park, MD 20742-4111, USA*
[3]*Center for Quantum Information, IIIS, Tsinghua University, Beijing 100084, PR China*
[4]*Department of Physics, Harvard University, Cambridge, Massachusetts 02138, USA*

(Dated: November 28, 2017)

S-1. STEREOGRAPHIC COORDINATES AND A SKETCH OF THE KNOTTED SPIN TEXTURE

For Hopf insulators in a cubic lattice, the first Brillouin zone (BZ) is a 3D torus $\mathbb{T}^3$. Since it is *not* convenient to draw and visualize different knots and links in $\mathbb{T}^3$, we first do a map g to go from $\mathbb{T}^3$ to $\mathbb{S}^3$ and use a stereographic coordinate system to represent $\mathbb{S}^3$. The stereographic projection used in this paper is defined as:

$$(x, y, z) = \frac{1}{1+\eta_4}(\eta_1, \eta_2, \eta_3), \tag{S1}$$

where (x, y, z) and $(\eta_1, \eta_2, \eta_3, \eta_4)$ are points of $\mathbb{R}^3$ and $\mathbb{S}^3$, respectively. In Fig.S1, we sketch the simplest nontrivial spin texture of Hopf insulators with $\chi(f) = 1$ in the stereographic coordinates defined above.

S-2. ADDING PERTURBATIONS TO THE HAMILTONIAN

In realistic experiments, there are additional noises other than the ideal Hamiltonian given by Eq.(3) in the main text. The first one is a weak global harmonic trap typically present in cold-atom experiment. It is of the form

$$H_{\text{trap}} = \frac{1}{2}m\omega^2 \sum_{\mathbf{r},\sigma} d_{\mathbf{r}}^2 c_{\mathbf{r},\sigma}^\dagger c_{\mathbf{r},\sigma}, \tag{S2}$$

where $\sigma = \uparrow, \downarrow$, m is the mass of the atom and $d_{\mathbf{r}}$ is the distance from the center of the trap to the lattice site $\mathbf{r}$. We use $\gamma_{\text{t}} = m\omega^2 a^2/2$ to parametrize the relative strength of the trap with a denoting the lattice constant. The other perturbation we consider is a random noise of the form

$$H_{\text{rand}} = \gamma_{\text{r}} \sum_{\mathbf{r},\mathbf{r}',\sigma,\sigma'} c_{\mathbf{r},\sigma}^\dagger \mathcal{R}_{\mathbf{r}\sigma,\mathbf{r}'\sigma'} c_{\mathbf{r}',\sigma'}, \tag{S3}$$

where γ_{r} characterizes the strength of the noise and $\mathcal{R}$ is a random Hermitian matrix with its largest eigenvalue normalized to unity.

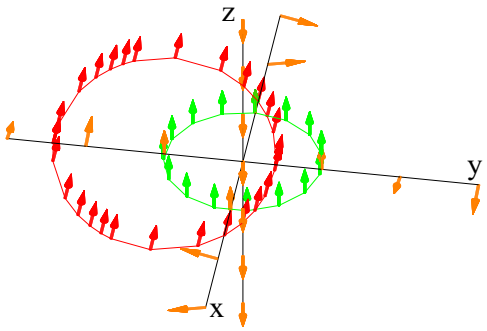

FIG. S1. Knotted spin texture in stereographic coordinates. We sketch the spin orientations along each axis and on two circles. The parameters are chosen as $p = q = 1$ and $h = 2$. Spins reside on the red (green) circle point to the x (z) direction and those on the z axis all point to the south (negative z direction). Also, all spins faraway from the origin asymptotically point to the south. This spin texture is nontrivial (twisted with $\chi(f) = 1$) and cannot be untwined continuously unless a topological phase transition is crossed.

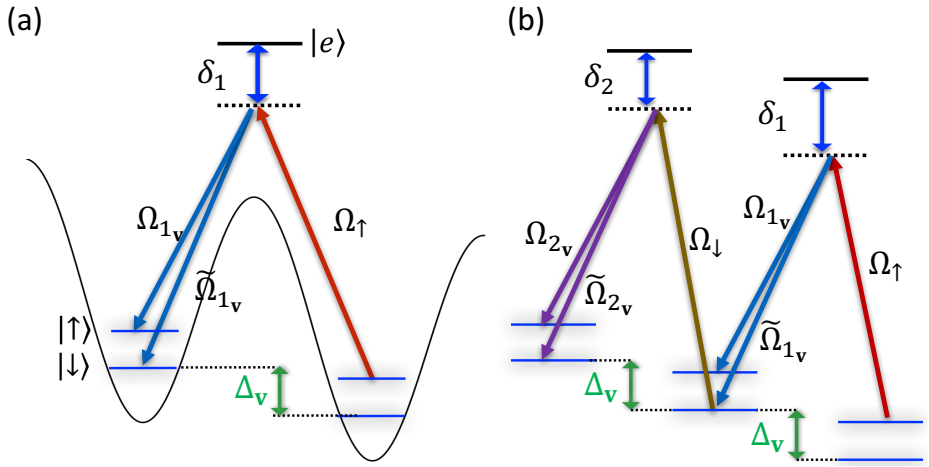

FIG. S2. Laser configurations: schematics of the laser configuration to realize the Hamiltonian $H_\mathbf{v}$. (a) A linear tilt $\Delta_\mathbf{v}$ per site along the $\mathbf{v}$ direction is imposed. A Raman triplet with detunings matching the frequency offset can induce spin-flip hoppings in a desired direction. (b) Two Raman triplets that realize all hoppings in $H_\mathbf{v}$. δ_1 and δ_2 are two different detunings from the excited states. The Rabi frequencies for each beam in terms of the unit Ω_0 are: $\widetilde{\Omega}_{1\mathbf{v}} = -\sqrt{2}\Omega_0 e^{i\pi/4}e^{-ikx}$, $\Omega_{1\mathbf{v}} = -\Omega_0 e^{-ikx}$, $\Omega_\uparrow = \Omega_0 e^{iky}$, $\widetilde{\Omega}_{2\mathbf{v}} = \sqrt{2}\Omega_0 e^{-i\pi/4}e^{-ikx}$, $\Omega_{2\mathbf{v}} = \Omega_0 e^{-ikx}$, and $\Omega_\downarrow = \Omega_0 e^{iky}$, where k is the magnitude of the laser wave vector. All these Raman beams can be draw from a single laser through an electric or acoustic optical modulator.

S-3. ϵ-NEIGHBORHOOD METHOD

As discussed in the main text, the spin orientation $\hat{\mathbf{S}}(\mathbf{k})$ in real experiment is always pixelized with a finite resolution. Therefore, for a specific orientation, $\hat{\mathbf{S}}_1$ for instance, the measured $\hat{\mathbf{S}}(\mathbf{k})$ can only be approximately rather than exactly equal to $\hat{\mathbf{S}}_1$ at any momentum point $\mathbf{k}$. Consequently, one need to consider a small ϵ-neighborhood of $\hat{\mathbf{S}}_1$:

$$N_\epsilon(\hat{\mathbf{S}}_1) = \{\hat{\mathbf{S}} : \ |\hat{\mathbf{S}} - \hat{\mathbf{S}}_1| \leq \epsilon\}, \tag{S4}$$

where $|\hat{\mathbf{S}} - \hat{\mathbf{S}}_1| = [(\hat{S}_x - \hat{S}_{1x})^2 + (\hat{S}_y - \hat{S}_{1y})^2 + (\hat{S}_z - \hat{S}_{1z})^2]^{1/2}$ measures the distance between $\hat{\mathbf{S}}$ and $\hat{\mathbf{S}}_1$. Let us denote the preimages of all orientations in $N_\epsilon(\hat{\mathbf{S}}_1)$ as a set $P_\epsilon(\hat{\mathbf{S}}_1) = (f \circ g)^{-1}[N_\epsilon(\hat{\mathbf{S}}_1)]$. With a finite resolution, the BZ is discrete and contains finite momentum points, and so does $P_\epsilon(\hat{\mathbf{S}}_1)$. As a result, one should wisely choose an appropriate value for ϵ so that $P_\epsilon(\hat{\mathbf{S}}_1)$ contains a proper amount of momentum points to depict the loop structure of $(f \circ g)^{-1}(\hat{\mathbf{S}}_1)$. To obtain Fig.3(b) in our numerical simulation in the main text, we examine the discrete $\hat{\mathbf{S}}(\mathbf{k})$ (observed from time-of-flight measurements) at each momentum point $\mathbf{k}$ and append $\mathbf{k}$ into the set $P_{1\epsilon}$ ($P_{2\epsilon}$) if $\hat{\mathbf{S}}(\mathbf{k})$ is in a ϵ-neighborhood of $\hat{\mathbf{S}}_1$ ($\hat{\mathbf{S}}_2$). Then Fig.3(b) can be obtained by plotting $g(P_{1\epsilon})$ and $g(P_{2\epsilon})$ in the stereographic coordinate system defined above.

S-4. REALIZING HOPF INSULATORS WITH COLD ATOMS

In the main text, we have been focused on how to measure the Hopf invariant and probe knots and links using the stardard time-of-flight imaging techniques. In this section, we propose a possible experimental scheme to realize Hopf insulators with ultracold atoms in optical lattices. For simplicity, we consider the case of $p = q = 1$. After a Fourier transform, the corresponding Hamiltonian in real space reads $H = H_{\text{sf}} + H_{\text{sp}}$, where H_{sf} denotes the collection of all terms with spin flips:

$$\begin{aligned} H_{\text{sf}} = \sum_{\mathbf{r}} \frac{1}{2}[&c^\dagger_{\mathbf{r},\uparrow}c_{\mathbf{r}+2\hat{x},\downarrow} - c^\dagger_{\mathbf{r},\uparrow}c_{\mathbf{r}-2\hat{x},\downarrow} - (1-i)c^\dagger_{\mathbf{r},\uparrow}c_{\mathbf{r}-\hat{x}-\hat{y},\downarrow} + (1+i)c^\dagger_{\mathbf{r},\uparrow}c_{\mathbf{r}+\hat{x}-\hat{y},\downarrow} - (1+i)c^\dagger_{\mathbf{r},\uparrow}c_{\mathbf{r}-\hat{x}+\hat{y},\downarrow} + ic^\dagger_{\mathbf{r},\uparrow}c_{\mathbf{r}-2\hat{y},\downarrow} \\ &+(1-i)c^\dagger_{\mathbf{r},\uparrow}c_{\mathbf{r}+\hat{x}+\hat{y},\downarrow} - ic^\dagger_{\mathbf{r},\uparrow}c_{\mathbf{r}+2\hat{y},\downarrow} - 2c^\dagger_{\mathbf{r},\uparrow}c_{\mathbf{r}-\hat{x}-\hat{z},\downarrow} + 2c^\dagger_{\mathbf{r},\uparrow}c_{\mathbf{r}+\hat{x}-\hat{z},\downarrow} + 2ic^\dagger_{\mathbf{r},\uparrow}c_{\mathbf{r}-\hat{y}-\hat{z},\downarrow} - 2ic^\dagger_{\mathbf{r},\uparrow}c_{\mathbf{r}+\hat{y}-\hat{z},\downarrow} \\ &+2h(c^\dagger_{\mathbf{r},\uparrow}c_{\mathbf{r}+\hat{x},\downarrow} - c^\dagger_{\mathbf{r},\uparrow}c_{\mathbf{r}-\hat{x},\downarrow} + ic^\dagger_{\mathbf{r},\uparrow}c_{\mathbf{r}-\hat{y},\downarrow} - ic^\dagger_{\mathbf{r},\uparrow}c_{\mathbf{r}+\hat{y},\downarrow})] + \text{h.c.}, \end{aligned}$$

and $H_{\rm sp}$ denotes the collection of all other terms:

$$\begin{aligned}H_{\rm sp}=\sum_{\mathbf{r}}\frac{1}{2}[&c^{\dagger}_{\mathbf{r},\downarrow}c_{\mathbf{r}-2\hat{x},\downarrow}+c^{\dagger}_{\mathbf{r},\downarrow}c_{\mathbf{r}+2\hat{x},\downarrow}+c^{\dagger}_{\mathbf{r},\downarrow}c_{\mathbf{r}+\hat{x}+\hat{y},\downarrow}+c^{\dagger}_{\mathbf{r},\downarrow}c_{\mathbf{r}-\hat{x}-\hat{y},\downarrow}+c^{\dagger}_{\mathbf{r},\downarrow}c_{\mathbf{r}-\hat{x}+\hat{y},\downarrow}+c^{\dagger}_{\mathbf{r},\downarrow}c_{\mathbf{r}+\hat{x}-\hat{y},\downarrow}+c^{\dagger}_{\mathbf{r},\downarrow}c_{\mathbf{r}-2\hat{y},\downarrow}\\&+c^{\dagger}_{\mathbf{r},\downarrow}c_{\mathbf{r}+2\hat{y},\downarrow}+c^{\dagger}_{\mathbf{r},\downarrow}c_{\mathbf{r}+\hat{x}+\hat{z},\downarrow}+c^{\dagger}_{\mathbf{r},\downarrow}c_{\mathbf{r}-\hat{x}-\hat{z},\downarrow}+c^{\dagger}_{\mathbf{r},\downarrow}c_{\mathbf{r}-\hat{x}+\hat{z},\downarrow}+c^{\dagger}_{\mathbf{r},\downarrow}c_{\mathbf{r}+\hat{x}-\hat{z},\downarrow}+c^{\dagger}_{\mathbf{r},\downarrow}c_{\mathbf{r}+\hat{y}+\hat{z},\downarrow}+c^{\dagger}_{\mathbf{r},\downarrow}c_{\mathbf{r}-\hat{y}-\hat{z},\downarrow}\\&+c^{\dagger}_{\mathbf{r},\downarrow}c_{\mathbf{r}-\hat{y}+\hat{z},\downarrow}+c^{\dagger}_{\mathbf{r},\downarrow}c_{\mathbf{r}+\hat{y}-\hat{z},\downarrow}+2h(c^{\dagger}_{\mathbf{r},\downarrow}c_{\mathbf{r}+\hat{x},\downarrow}+c^{\dagger}_{\mathbf{r},\downarrow}c_{\mathbf{r}-\hat{x},\downarrow}+c^{\dagger}_{\mathbf{r},\downarrow}c_{\mathbf{r}+\hat{y},\downarrow}+c^{\dagger}_{\mathbf{r},\downarrow}c_{\mathbf{r}-\hat{y},\downarrow}\\&+c^{\dagger}_{\mathbf{r},\downarrow}c_{\mathbf{r}+\hat{z},\downarrow}+c^{\dagger}_{\mathbf{r},\downarrow}c_{\mathbf{r}-\hat{z},\downarrow})+2(1+h^2)c^{\dagger}_{\mathbf{r},\downarrow}c_{\mathbf{r},\downarrow}]-[\downarrow\to\uparrow].\end{aligned}$$

To realize Hopf insulators with ultracold atoms, the method used here is similar to that in Ref. [1], where a cold-atom implementation of three-dimensional (3D) chiral topological insulators was proposed. We consider cold fermionic atoms (^{6}Li for example) in a 3D cubic optical lattice and choose two internal atomic levels (hyperfine states) as our spin states $|\uparrow\rangle$ and $|\downarrow\rangle$. Other levels are initially depopulated by optical pumping and transitions to those levels are forbidden due to a large energy detuning or carefully selected laser polarizations. In real space, the Hamiltonian has spin-orbit coupled hoppings along nine possible directions. Here, we explicitly demonstrate how to engineer the specific hoppings along the $\mathbf{v}=\hat{x}+\hat{y}$ direction. For other directions, the realization scheme will be similar and thus omitted for conciseness. The hopping terms in the $\mathbf{v}$ direction can be written as

$$H_{\mathbf{v}}=\frac{1}{2}\sum_{\mathbf{r}}[-(1+i)c^{\dagger}_{\mathbf{r},\downarrow}-c^{\dagger}_{\mathbf{r},\uparrow}]c_{\mathbf{r}+\mathbf{v},\uparrow}+[(1-i)c^{\dagger}_{\mathbf{r},\uparrow}+c^{\dagger}_{\mathbf{r},\downarrow}]c_{\mathbf{r}+\mathbf{v},\downarrow}+\text{h.c.} \tag{S5}$$

Apparently, $H_{\mathbf{v}}$ consists of various hopping terms coupled with spin rotations. Basically, both spin $|\uparrow\rangle$ and $|\downarrow\rangle$ hop along the $-\mathbf{v}$ direction to become a superposition of both spin states. We can decompose the four different hopping terms and each of them can be achieved via Raman-assisted tunnelings [2–4]. For instance, the first two hoppings can be activated by two Raman pairs, $\Omega_{\uparrow}$, $\widetilde{\Omega}_{1\mathbf{v}}$, and $\Omega_{\uparrow}$, $\Omega_{1\mathbf{v}}$, where $\Omega_{\uparrow}$ is in common; $\widetilde{\Omega}_{1\mathbf{v}}$ and $\Omega_{1\mathbf{v}}$ can be drawn from the same beam split by an electric or acoustic optical modulator. The phase and strength of the hopping can be controlled by the laser phase and intensity (see caption of Fig. S2). Similarly, the other two hopping terms can be triggered by the Raman triplet $\widetilde{\Omega}_{2\mathbf{v}}$, $\Omega_{2\mathbf{v}}$ and $\Omega_{\downarrow}$ as shown in Fig. S2.

One may notice that the parity (left-right) symmetry is explicitly broken and natural hoppings are suppressed. Both of these can be achieved by a homogeneous energy gradient along the $\mathbf{v}$ direction, which can be accomplished, for instance, by the magnetic field gradient, dc- or ac-Stark shift gradient, or the natural gravitational field [1, 3, 4]. We denote the linear energy shift per site in the $\mathbf{v}$ direction by $\Delta_{\mathbf{v}}$ and impose that natural tunneling rate $t_0\ll\Delta_{\mathbf{v}}$. As a consequence, the natural tunneling probability $(t_0/\Delta_{\mathbf{v}})^2$ is negligible in this tilted lattice. The energy offset also forbids Raman-assisted tunnelings in the opposite direction other than the ones prescribed above. Incommensurate tilts along different directions also suppress unwanted couplings among them. The detuning δ_1 and δ_2 for the two Raman triplets should also be different, so that no unintended interference between these two triplets happens. In addition, the wave-vector difference of two Raman beams $\delta\mathbf{k}$ has to have a component along the hopping direction ($\mathbf{v}$-direction in this case) to ensure the Raman-assisted hopping strength is non-vanishing [1].

Since the real-space Hamiltonian contains hopping terms along nine different directions and each of them requires a similar configuration as above, the overall scheme necessitates a considerable number of laser beams. Although many of the beams can be used in common and created from the same laser by an electric or acoustic optical modulator, the implementation is nonetheless very challenging. A simpler implementation protocol of Hopf insulators is highly desired. Controlled periodic driving may be a promising alternative. Also, theoretically it may be possible to find a more natural model Hamiltonian that encapsulates the nontrivial Hopf physics, which may in turn simplify the experimental realization. We would like to emphasize, however, our detection and measurement protocol do not depend on the particular realization scheme. Regardless of the specific implementation of Hopf Hamiltonians, we can detect the Hopf invariant and probe the rich knot structures hidden in Hopf insulators.

* dldeng15@umd.edu

[1] Wang S T, Deng D L, and Duan L M, 2014 Phys. Rev. Lett. **113** 033002.
[2] Jaksch D and Zoller P, 2003 New J. Phys. **5** 1 56.
[3] Miyake H, Siviloglou G A, Kennedy C J, Burton W C, and Ketterle W, 2013 Phys. Rev. Lett. **111** 185302.
[4] Aidelsburger M, Atala M, Lohse M, Barreiro J T, Paredes B, and Bloch I, 2013 Phys. Rev. Lett. **111** 185301.